



TssA from *Burkholderia cenocepacia*: expression, purification, crystallization and crystallographic analysis

Hayley J. Owen,^{a‡} Ruyue Sun,^{b‡} Asma Ahmad,^{b‡} Svetlana E. Sedelnikova,^a Patrick J. Baker,^a Mark S. Thomas^{b*} and David W. Rice^{a*}

Received 16 May 2018

Accepted 6 July 2018

Edited by R. L. Stanfield, The Scripps Research Institute, USA

‡ These authors contributed equally.

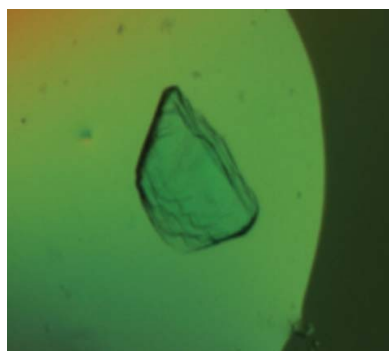
Keywords: type VI secretion system; TssA; *Burkholderia cenocepacia*.

^aDepartment of Molecular Biology and Biotechnology, Krebs Institute, University of Sheffield, Western Bank, Sheffield S10 2TN, England, and ^bDepartment of Infection, Immunity and Cardiovascular Disease, University of Sheffield Medical School, Beech Hill Road, Sheffield S10 2RX, England. *Correspondence e-mail: m.s.thomas@sheffield.ac.uk, d.rice@sheffield.ac.uk

TssA is a core component of the type VI secretion system, and phylogenetic analysis of TssA subunits from different species has suggested that these proteins fall into three distinct clades. Whilst representatives of two clades, TssA1 and TssA2, have been the subjects of investigation, no members of the third clade (TssA3) have been studied. Constructs of TssA from *Burkholderia cenocepacia*, a representative of clade 3, were expressed, purified and subjected to crystallization trials. Data were collected from crystals of constructs of the N-terminal and C-terminal domains. Analysis of the data from the crystals of these constructs and preliminary structure determination indicates that the C-terminal domain forms an assembly of 32 subunits in D_{16} symmetry, whereas the N-terminal domain is not involved in subunit association.

1. Introduction

The type VI secretion system (T6SS) is composed of 14 core components, TssA–TssM and PAAR, which together form a contractile machine that injects protein effectors into target cells (Pukatzki *et al.*, 2007; Shalom *et al.*, 2007; Zheng & Leung, 2007; Boyer *et al.*, 2009; Leiman *et al.*, 2009; Cianfanelli *et al.*, 2016). The core components form a number of sub-complexes, including the sheath/tube complex, membrane complex and baseplate (Leiman *et al.*, 2009; Basler *et al.*, 2012; Shneider *et al.*, 2013; Brunet *et al.*, 2015; Durand *et al.*, 2015). TssB and TssC form the contractile sheath, which surrounds the TssD inner tube (Bönemann *et al.*, 2009; Leiman *et al.*, 2009; Basler *et al.*, 2012; Brunet *et al.*, 2014). TssI and PAAR sit on top of the tube and may be decorated with covalently or noncovalently attached effector proteins (Pukatzki *et al.*, 2007; Leiman *et al.*, 2009; Shneider *et al.*, 2013). Upon contraction of the sheath against the baseplate, the tube, which can also carry effector proteins, passes through the baseplate and is ejected from the cell (Pukatzki *et al.*, 2006; Basler *et al.*, 2012; Silverman *et al.*, 2013). TssH then acts to recycle the sheath components post-contraction for reassembly in the extended state (Bönemann *et al.*, 2009; Basler *et al.*, 2012; Kapitein *et al.*, 2013). TssJ, TssL and TssM form a complex that anchors the contractile machinery to the cell envelope through interactions with the baseplate (Aschtgen *et al.*, 2010; Zoued *et al.*, 2013; Brunet *et al.*, 2015; Durand *et al.*, 2015). TssE, TssF, TssG and TssK are components of the baseplate, which serves as a



OPEN ACCESS

Table 1
Construct information.

Construct	His ₆ -TssA Nt1	MBP-TssA CTD
B.c TssA amino acids	1–255	303–373
Tag details	MGSSHHHHHSSGLVPRGSH	(MBP) NSSSSNNNNNNNNNLGIEGR / ISHM†
Construct sequence	<u>MGSSHHHHHSSGLVPRGSH</u> <u>M</u> PINLPELLTPISEASPSGDDLLFSNE FDAIQDARRYDDPTLDQGEWVTEIKEADWGFVVDHAGELLRTRTKDL RLAVWLTEALALEDGITGLTEGYALLEGLCREFDWTFHPLPEDDDIE HRLGNVAWLSGRTAELLRAVPLTDGASNAFSTLDWEVAQHVAQSIKR DPEHADDIARGKPSIEQIDASRRVTSIAFYTALLANLKAFFALDAF EERLVERAGDSAPFRQARDAFETVYRLAERFAREQGYTG	<u>(MBP) NSSSSNNNNNNNNNLGIEGR / ISHMI</u> <u>Q</u> NRQAQVDQLRAVAR YFRQTEPHSPVAYLADKAAEWADMPLHKWLESVVKDDGSLSHIR ELLGVRPDEQS
Forward primer‡	pET-14b-iotAfor, GCGC CATATG CCGATCAATCTCCCCGA	pET-14b-ACTDfor3, GCGC CATATG ATCCAGAACCGTGCCGAGGC
Reverse primer‡	pET-14b-TssA-NTDrev, GCGC GGATCC TTAGCCGGTATAGCCCT GTTCGC	pET-14b-iotArev, GCGC GGATCC TGCGTTTACGACTGCTCGTC
Restriction enzymes	NdeI and BamHI	NdeI and BamHI
Expression vector	pET-14b	pMAL-c5X
Antibiotic	100 µg ml ⁻¹ ampicillin	100 µg ml ⁻¹ ampicillin
Expression host	<i>E. coli</i> BL21 (DE3)	<i>E. coli</i> ER2523 (NEB Express)

† MBP is maltose-binding protein; IEGR is the Factor Xa recognition site; / indicates the Factor X cleavage site. Tags are highlighted as underlined regions of the construct sequences. ‡ Bold sequences indicate restriction sites. Translation initiation and termination codons are underlined.

platform for priming of the sheath and tube assembly (Basler *et al.*, 2012; English *et al.*, 2014; Brunet *et al.*, 2015).

Following phylogenetic analysis, TssA proteins have been classified into three clades (TssA1–TssA3; Planamente *et al.*, 2016), with representative TssAs belonging to clades TssA1 (PA0082 from *Pseudomonas aeruginosa*; Pa TssA1) and TssA2 (Ec042_4540 from enteroaggregative *Escherichia coli*; E.c TssA2) having previously been the subject of biochemical and structural studies (Planamente *et al.*, 2016; Zoued *et al.*, 2016). The Pa and E.c TssAs have been shown to interact with the T6SS sheath, inner tube and components of the baseplate, with E.c TssA2 also interacting with the membrane complex (Planamente *et al.*, 2016; Zoued *et al.*, 2016). Pa TssA1 is proposed to contain two domains which form a ring structure comprising the C-terminal domain with a flexible peripheral N-terminal domain (Planamente *et al.*, 2016). Similarly, in E.c TssA2 the C-terminal domain oligomerizes to produce a dodecameric structure of two stacked rings with *D*₆ symmetry (Zoued *et al.*, 2016). In E.c TssA2 the N-terminal region is predicted to form arms which extend out from the C-terminal dodecamer core (Zoued *et al.*, 2016). The structure of part of the E.c TssA2 N-terminal region, Nt2, forms a dimer (Zoued *et al.*, 2016). Bioinformatic analysis identified a conserved region within both the Pa TssA1 and E.c TssA2 N-terminal domains, referred to as ImpA_N (Planamente *et al.*, 2016; Zoued *et al.*, 2017). Pa TssA1 was observed to localize at one end of the sheath, whilst E.c TssA2 was seen to move away from an initial site at the membrane concomitant with sheath polymerization (Planamente *et al.*, 2016; Zoued *et al.*, 2016). Based on these observations of Pa TssA1 and some low-level predicted similarities in secondary structure, it was suggested that the TssA1 C-terminal region corresponds to the C-terminal region of the phage T4 baseplate component gp6, thereby identifying Pa TssA1 as a possible baseplate component (Planamente *et al.*, 2016). On the other hand, E.c TssA2 was predicted to be involved in recruitment of the baseplate assembly to the membrane complex and subsequent poly-

merization of the TssD tube and TssB/TssC sheath (Zoued *et al.*, 2016).

Burkholderia cenocepacia TssA (B.c TssA), locus tag I35_RS01755, is a member of TssA3, the TssA clade that has yet to be investigated (Planamente *et al.*, 2016). In this paper, we describe the production of constructs of B.c TssA representing the predicted N-terminal and C-terminal domains. Overexpression of the domains, their purification and their crystallization resulted in the production of diffraction-quality crystals, analysis of which provides preliminary information on their stoichiometry, symmetry and structural organization.

2. Materials and methods

2.1. Macromolecule production

Coding sequences for the predicted N-terminal domain (Nt1) and C-terminal domain (CTD) of B.c TssA (UniProt A0A1V2WLD6) were amplified from *B. cenocepacia* strain H111 (Römling *et al.*, 1994) by PCR using the appropriate combinations of primers as shown in Table 1. The DNA products were ligated to either plasmid pET-14b (Novagen; encoding a His₆ purification tag and a thrombin cleavage site) or pMAL-c5X [NEB; encoding a maltose-binding protein (MBP) solubility tag and a Factor Xa cleavage site], followed by transformation of *E. coli* strain JM83 (Yanisch-Perron *et al.*, 1985). Construct details are shown in Table 1.

A B.c His₆-TssA Nt1 construct was overexpressed in *E. coli* BL21 (DE3) cells (Studier & Moffatt, 1986) grown in brain heart infusion broth (Becton Dickinson) at 37°C to an OD₆₀₀ of 0.5–0.7, whereupon expression was induced by the addition of 1 mM IPTG followed by incubation for a further 2–3 h. B.c His₆-TssA Nt1 was purified from clarified cell lysate in 50 mM Tris pH 8.0, 500 mM NaCl, applied onto a HisTrap HP column (GE Healthcare Life Sciences) and eluted with a linear gradient of imidazole (0–350 mM) in 50 mM Tris pH 8.0, 500 mM NaCl. Fractions containing the B.c His₆-TssA Nt1

Table 2
Crystallization.

Construct	His ₆ -TssA Nt1	TssA CTD	SeMet-TssA CTD
Method	Sitting-drop vapour diffusion	Sitting-drop vapour diffusion	Hanging-drop vapour diffusion
Composition of reservoir solution	0.16 M calcium acetate, 0.08 M sodium cacodylate buffer pH 6.5, 14.4%(w/v) PEG 8000, 20%(v/v) glycerol	0.1 M sodium chloride, 0.1 M Tris pH 8.0, 15%(v/v) ethanol, 5%(v/v) MPD	1 M ammonium sulfate, 2%(w/v) PEG 3350, 0.1 M bis-tris pH 6.0
Volume and ratio of drop	200 nl:200 nl	200 nl:200 nl	2 µl:1 µl (protein:reservoir)
Volume of reservoir (µl)	50	50	1000

Table 3
Data-collection and processing statistics.

Values in parentheses are for the highest resolution shell.

Construct	His ₆ -TssA Nt1	His ₆ -TssA Nt1 + iodine	TssA CTD	SeMet-TssA CTD
Wavelength (Å)	0.92000	1.70000	0.97949	0.97922
Beamline	I04-1	I03	I04	I03
Detector	PILATUS 2M	PILATUS 6M	PILATUS 6M-F	PILATUS3 6M
Rotation range per image (°)	0.2	0.2	0.2	0.1
Total rotation range (°)	90	720	180	360
Exposure time per image (s)	0.2	0.2	0.2	0.05
Data-processing package	<i>xia2 -3daii</i>	<i>fast_dp</i>	<i>xia2 -3daii</i>	<i>xia2 -3d</i>
Space group	<i>P2₁2₁2</i>	<i>P2₁2₁2</i>	<i>I222</i>	<i>I222</i>
<i>a</i> , <i>b</i> , <i>c</i> (Å)	49.7, 125.4, 45.5	45.6, 49.8, 126.1	46.9, 203.0, 267.9	46.3, 201.3, 263.9
α , β , γ (°)	90.0, 90.0, 90.0	90.0, 90.0, 90.0	90.0, 90.0, 90.0	90.0, 90.0, 90.0
Resolution range (Å)	62.69–1.87 (1.92–1.87)	29.68–2.01 (2.06–2.01)	55.90–3.79 (3.89–3.79)	80.61–2.86 (2.93–2.86)
<i>R</i> _{merge}	0.067 (0.495)	0.131 (0.761)	0.221 (0.871)	0.207 (2.520)
<i>R</i> _{p.i.m.}	0.051 (0.372)	0.031 (0.174)	0.112 (0.487)	0.064 (0.747)
$\langle I/\sigma(I) \rangle$	10.8 (2.0)	20.6 (3.4)	7.6 (2.0)	11.1 (1.1)
Completeness (%)	98.4 (99.3)	98.4 (79.0)	99.4 (99.7)	100.0 (100.0)
Multiplicity	3.3 (3.3)	23.0 (18.7)	5.7 (5.3)	13.0 (13.2)
Total reflections	77962	448717	75744	382400
Unique reflections	23839	19523	13207	29304

protein were concentrated using a 30 kDa molecular-weight cutoff concentrator and washed with 10 mM Tris pH 8.0 for crystallization.

The B.c MBP-TssA CTD fusion protein was overproduced in *E. coli* ER2523 cells (NEB Express) grown in Lennox broth containing 0.2% glucose (Lennox, 1955) at 37°C to an OD₆₀₀ of 0.6–0.7, whereupon protein overexpression was induced with 0.3 mM IPTG and incubation of the culture continued at the same temperature for a further 2–3 h. To prepare selenomethionine-incorporated B.c MBP-TssA CTD protein (B.c SeMet-MBP-TssA CTD), 2 × 500 ml of cells were grown as described above and harvested prior to induction. The cell pellets were then resuspended in selenomethionine minimal medium, harvested and the resuspension was added to 2 × 500 ml selenomethionine minimal medium [10.5 g l⁻¹ K₂HPO₄, 1.0 g l⁻¹ (NH₄)₂SO₄, 4.5 g l⁻¹ KH₂PO₄, 0.5 g l⁻¹ trisodium citrate-2H₂O, 5.0 g l⁻¹ glycerol and 0.5 g l⁻¹ each of adenine, guanosine, thymine and uracil] supplemented with 1.0 g l⁻¹ MgSO₄·7H₂O, 4.0 mg l⁻¹ thiamine, 100 mg l⁻¹ each of L-lysine, L-phenylalanine and L-threonine, 50 mg l⁻¹ each of L-isoleucine, L-leucine and L-valine, 40 mg l⁻¹ seleno-L-methionine and 2.0 g l⁻¹ glucose. Growth was continued for 1 h at 37°C prior to the induction of B.c MBP-TssA CTD expression by the addition of 0.3 mM IPTG and subsequent growth at 37°C overnight.

Harvested B.c MBP-TssA CTD- and B.c SeMet-MBP-TssA CTD-overexpressing cells were each resuspended in column-

binding buffer (50 mM Tris-HCl pH 8.0, 200 mM NaCl) and the cells were lysed by sonication. The cell lysate was cleared by centrifugation before being applied onto amylose resin (NEB) equilibrated with column-binding buffer. After washing the resin with column-binding buffer, the bound material was then eluted in the same buffer with the addition of 10 mM maltose. Fractions containing the fusion protein were concentrated and then digested with Factor Xa (5 µg per milligram of protein; NEB) in the presence of 2 mM CaCl₂ at room temperature for ~14 h to release the target protein from MBP. Following cleavage of the MBP, the products were separated by gel filtration on a Superdex 200 column (GE Healthcare Life Sciences) in 50 mM Tris-HCl pH 8.0, 500 mM NaCl. The B.c TssA CTD protein obtained from gel filtration was applied to a final amylose column to remove any uncleaved B.c MBP-TssA CTD fusion molecules. This step was added to avoid heterogeneity of the sample. The protein was then concentrated and buffer-exchanged into 5 mM Tris-HCl pH 8.0, 50 mM NaCl for crystallization. The purified B.c TssA CTD protein has an additional four non-native residues (ISHM) at the N-terminus following proteolytic release from the N-terminal MBP solubility tag (Table 1).

2.2. Crystallization

B.c TssA protein constructs were set down into sitting-drop crystallization trials using a Matrix Hydra II Plus One robot,

with 200 nl:200 nl drops and a 50 μ l reservoir, or hanging-drop crystallization trials, and stored at 17°C. A selection of crystallization condition suites were used for screening, including JCSG+, ProPlex, PACT, Classics, MPD, AmSO₄, PEGs and pHClear (Qiagen, Molecular Dimensions). B.c His₆-TssA Nt1 crystals grew in sitting-drop trial conditions consisting of 0.16 M calcium acetate, 0.08 M sodium cacodylate buffer pH 6.5, 14.4% (w/v) PEG 8000, 20% (v/v) glycerol. B.c TssA CTD produced crystals in sitting-drop trial conditions consisting of 0.1 M sodium chloride, 0.1 M Tris pH 8.0, 15% (v/v) ethanol, 5% (v/v) MPD. B.c SeMet-TssA CTD produced crystals in hanging-drop trial conditions consisting of 1 M ammonium sulfate, 2% (w/v) PEG 3350, 0.1 M bis-tris pH 6.0. Crystallization information is shown in Table 2.

2.3. Data collection, processing and analysis

Data were collected from B.c His₆-TssA Nt1 crystals [cryoprotected in 0.16 M calcium acetate, 0.08 M sodium cacodylate buffer pH 6.5, 16.4% (w/v) PEG 8000, 30% (v/v) glycerol] on beamline I04-1 at Diamond Light Source. The data were processed to 1.87 Å resolution using the *-3daii* option in *xia2* (Collaborative Computational Project, Number 4, 1994; Evans, 2006; Kabsch, 2010; Winter, 2010) and indicated that the crystals belonged to space group *P2₁2₁2* (unit-cell parameters $a = 49.7$, $b = 125.4$, $c = 45.5$ Å). Data-collection and processing statistics are shown in Table 3.

Data were collected from B.c TssA CTD crystals [cryoprotected in 0.1 M sodium chloride, 0.1 M Tris pH 8.0, 15% (v/v) ethanol, 25% (v/v) glycerol] on beamline I04 at Diamond Light Source. Data were processed to 3.79 Å resolution using the *-3daii* option in *xia2* (Collaborative Computational Project, Number 4, 1994; Sauter *et al.*, 2004; Evans, 2006; Zhang *et al.*, 2006; Kabsch, 2010; Winter, 2010) and indicated that the crystals belonged to space group *I222*. Data-collection and processing statistics are shown in Table 3. A self-rotation function was calculated on all of the data from crystals of B.c TssA CTD using an integration radius of 44 Å in *POLARRFN* (Winn *et al.*, 2011). Self Patterson functions on the native data were calculated using *FFT for Patterson* (Winn *et al.*, 2011).

B.c His₆-TssA Nt1 crystals were subjected to the sublimation of elemental iodine for ~3 h prior to cryoprotection in 0.16 M calcium acetate, 0.08 M sodium cacodylate buffer pH 6.5, 16.4% (w/v) PEG 8000, 30% (v/v) glycerol and data collection on beamline I03 at Diamond Light Source. The data were processed to 2.01 Å resolution with *fast_dp* (Winter

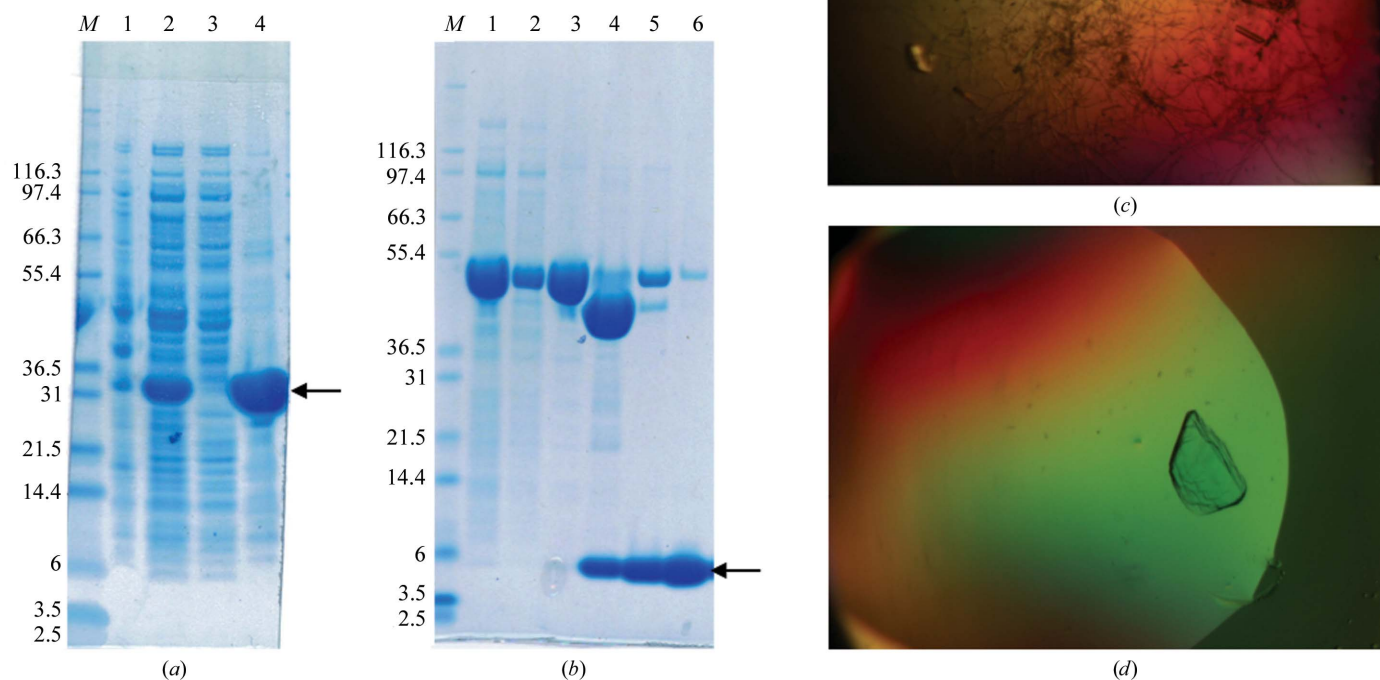


Figure 1

(a) SDS-PAGE analysis of protein purification of the B.c His₆-TssA Nt1 construct. Lane M, Mark12 marker (labelled in kDa). Lane 1, cell debris. Lane 2, cell-free extract. Lane 3, flowthrough (Ni column). Lane 4, final preparation. (b) SDS-PAGE analysis of protein purification of the B.c SeMet MBP-TssA CTD construct. The protein, indicated by the arrow, is shown to be ~90% pure in the final preparation samples and thus was used for crystallization. Lane M, Mark12 marker (labelled in kDa). Lane 1, cell-free extract. Lane 2, unbound material (amylose column). Lane 3, B.c SeMet MBP-TssA CTD. Lane 4, after MBP cleavage. Lane 5, after gel filtration. Lane 6, final preparation. (c) B.c His₆-TssA Nt1 crystals grown in 0.16 M calcium acetate, 0.08 M sodium cacodylate buffer pH 6.5, 14.4% (w/v) PEG 8000, 20% (v/v) glycerol. (d) B.c TssA CTD crystals grown in 0.1 M sodium chloride, 0.1 M Tris pH 8.0, 15% (v/v) ethanol, 5% (v/v) MPD.

& McAuley, 2011) and indicated that the crystals belonged to space group $P2_12_12$ (unit-cell parameters $a = 45.6$, $b = 49.8$, $c = 126.1$ Å). Data-collection statistics are shown in Table 3.

Data were collected from B.c SeMet-TssA CTD crystals [cryoprotected in 1–1.2 M ammonium sulfate, 3–4% (w/v) PEG 3350, 0.1 M bis-tris pH 6.0, 30% (v/v) glycerol] on beamline I03 at Diamond Light Source. The data were processed to 2.86 Å resolution using the $-3d$ option in *xia2* (Collaborative Computational Project, Number 4, 1994; Evans, 2006; Kabsch, 2010; Winter, 2010) and indicated that the crystals belonged to space group $I222$ (unit-cell parameters $a = 46.3$, $b = 201.3$, $c = 263.9$ Å). Data-collection statistics are shown in Table 3.

3. Results and discussion

3.1. Construct design

The design of the constructs for the N- and C-terminal domains of B.c TssA was based on an analysis of the pattern of sequence conservation across the different clades of TssA and resulted in stable, soluble samples of the proteins encoded by these regions of the gene. Constructs of the predicted N-terminal domain (Nt1) and C-terminal domain (CTD) of B.c TssA produced crystals (Fig. 1) which diffracted to high resolution.

3.2. TssA data analysis

Analysis of the Matthews coefficient of the B.c His₆-TssA Nt1 crystals suggests that the crystals contain one molecule of ~30.7 kDa in the asymmetric unit, with a V_M of $2.31 \text{ \AA}^3 \text{ Da}^{-1}$

(Matthews, 1968; Kantardjieff & Rupp, 2003; Winn *et al.*, 2011). In contrast, the contents of the asymmetric unit of the B.c TssA CTD crystals could not be confidently assigned from analysis of the Matthews coefficient. Consideration of possible values of V_M suggests that the asymmetric unit contains between nine and 21 subunits (4.13 – $1.77 \text{ \AA}^3 \text{ Da}^{-1}$; Matthews, 1968; Kantardjieff & Rupp, 2003; Winn *et al.*, 2011). It has previously been reported that the TssA CTD acts as an oligomerization domain which produces ring-like or star-like structures, as has been shown for Pa TssA1 and E.c TssA2, respectively (Planamente *et al.*, 2016; Zoued *et al.*, 2016). Self Pattersons calculated using the native data to 6 or 3.79 Å resolution showed no significant peaks above 15% of the origin, consistent with the absence of translational symmetry in the crystal. A self-rotation function was calculated on the B.c TssA CTD data using an integration radius of 44 Å to detect the presence of noncrystallographic symmetry. This identified peaks on the $\kappa = 180^\circ$ section with a height of approximately 70% of the origin corresponding to twofold axes located in the bc plane every 11.25° (Fig. 2). Consideration of the rotational symmetry and apparent molecular weight, determined by gel-filtration analysis (Fig. 2), suggests that the quaternary structure of B.c TssA CTD is composed of 32 subunits in D_{16} symmetry. This suggests that the asymmetric unit contains eight subunits with an unusually high V_M ($4.64 \text{ \AA}^3 \text{ Da}^{-1}$; Matthews, 1968; Kantardjieff & Rupp, 2003; Winn *et al.*, 2011). A preliminary electron-density map was calculated using SAD data to 2.86 Å resolution from the selenomethionine derivative of the B.c TssA CTD crystals, with an initial chain trace confirming the presence of B.c TssA CTD in the crystals and the nature of the symmetry indicated

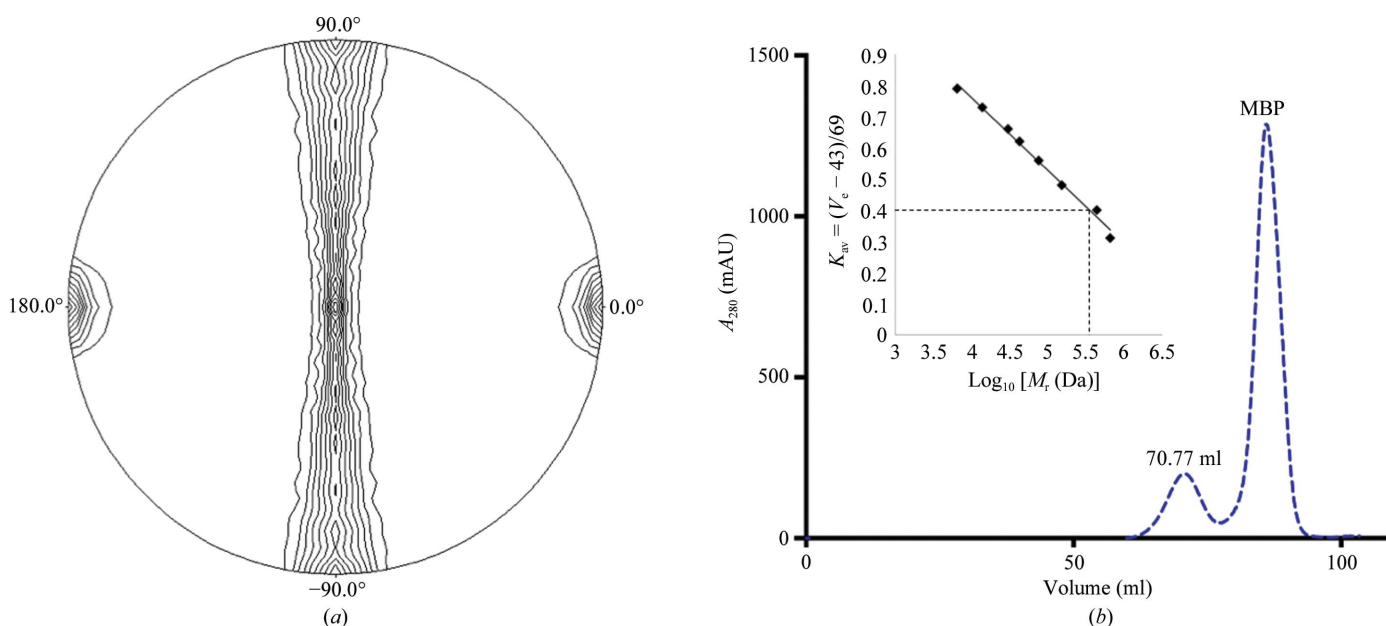


Figure 2
 (a) The self-rotation function for B.c TssA CTD crystals calculated on all data from 55.90 to 3.79 Å resolution using a 44 Å radius of integration. The section shown corresponds to $\kappa = 180^\circ$, with the orthogonal x , y and z axes along the crystallographic a , b and c axes, respectively. Noncrystallographic twofold axes can be seen every 11.25° in the bc plane at approximately 70% of the origin. The image was generated in *POLARRFN* (Winn *et al.*, 2011).
 (b) Gel-filtration chromatogram of B.c SeMet-MBP-TssA CTD protein, with UV absorption (280 nm) shown as a dotted blue line and the elution volume (70.77 ml) corresponding to B.c TssA CTD shown above the curve. Inset: calibration curve for the gel-filtration column, with $K_{av} = 0.4$ ($V_c = 70.77$ ml) highlighted corresponding to a molecular mass of $\sim 3.55 \times 10^5$ Da for B.c TssA CTD.

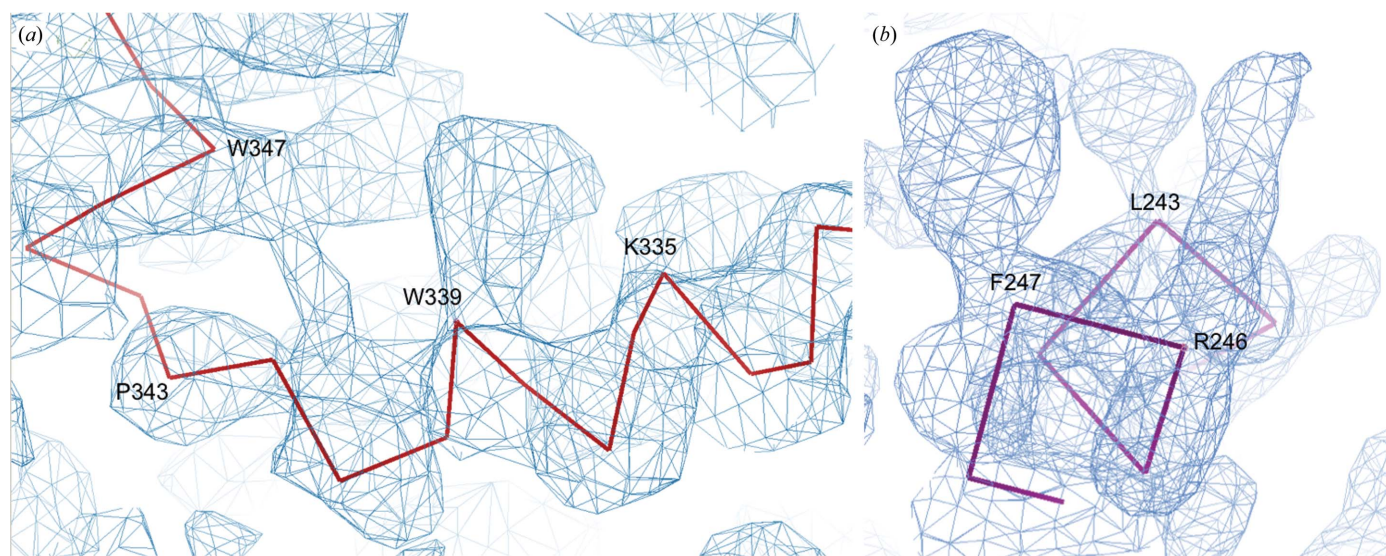


Figure 3

Preliminary electron-density maps, contoured at $\sim 1.0\sigma$, representing (a) a helical section of B.c TssA CTD. The large side chain visible towards the C-terminal end of the helix corresponds to Trp339, and density can also be seen for the nearby Trp347. Phases were obtained from *SHELX* (Sheldrick, 2008). (b) A helical section of the B.c His₆-TssA Nt1 domain. The large side chain visible at the C-terminal end of the helix corresponds to Phe247, and density can also be seen for the side chain of the adjacent Arg246. Phases were obtained from *fast_ep* and *SHELX* (Sheldrick, 2008). Images were generated in *Coot* (Emsley *et al.*, 2010).

by the self-rotation function (Fig. 2). Similarly, a preliminary electron-density map has been calculated using SAD data to 2.01 Å resolution from iodine-exposed B.c His₆-TssA Nt1 crystals (Fig. 3). Refinement of the structures and attempts to extend the resolution of the data are ongoing.

Acknowledgements

We would like to thank Diamond Light Source and the beamline scientists for access to beamlines I03, I04 and I04-1 and support during data collection.

Funding information

BBSRC Doctoral Training Grant (Grant No. BB/J014443/1 to Hayley J. Owen); Libyan Ministry of Higher Education (Scholarship to Asma Ahmad).

References

- Aschtgen, M.-S., Gavioli, M., Dessen, A., Lloubès, R. & Cascales, E. (2010). *Mol. Microbiol.* **75**, 886–899.
- Basler, M., Pilhofer, M., Henderson, G. P., Jensen, G. J. & Mekalanos, J. J. (2012). *Nature (London)*, **483**, 182–186.
- Bönemann, G., Pietrosiuk, A., Diemand, A., Zentgraf, H. & Mogk, A. (2009). *EMBO J.* **28**, 315–325.
- Boyer, F., Fichant, G., Berthod, J., Vandenbrouck, Y. & Attree, I. (2009). *BMC Genomics*, **10**, 104.
- Brunet, Y. R., Hénin, J., Celia, H. & Cascales, E. (2014). *EMBO Rep.* **15**, 315–321.
- Brunet, Y. R., Zoued, A., Boyer, F., Douzi, B. & Cascales, E. (2015). *PLOS Genet.* **11**, e1005545.
- Cianfanelli, F. R., Alcoforado Diniz, J., Guo, M., De Cesare, V., Trost, M. & Coulthurst, S. J. (2016). *PLoS Pathog.* **12**, e1005735.
- Collaborative Computational Project, Number 4 (1994). *Acta Cryst. D* **50**, 760–763.

- Durand, E., Nguyen, V. S., Zoued, A., Logger, L., Péhau-Arnaudet, G., Aschtgen, M. S., Spinelli, S., Desmyter, A., Bardiaux, B., Dujancourt, A., Roussel, A., Cambillau, C., Cascales, E. & Fronzes, R. (2015). *Nature (London)*, **523**, 555–560.
- Emsley, P., Lohkamp, B., Scott, W. G. & Cowtan, K. (2010). *Acta Cryst. D* **66**, 486–501.
- English, G., Byron, O., Cianfanelli, F. R., Prescott, A. R. & Coulthurst, S. J. (2014). *Biochem. J.* **461**, 291–304.
- Evans, P. (2006). *Acta Cryst. D* **62**, 72–82.
- Kabsch, W. (2010). *Acta Cryst. D* **66**, 125–132.
- Kantardjieff, K. A. & Rupp, B. (2003). *Protein Sci.* **12**, 1865–1871.
- Kapitein, N., Bönemann, G., Pietrosiuk, A., Seyffer, F., Hausser, I., Locker, J. K. & Mogk, A. (2013). *Mol. Microbiol.* **87**, 1013–1028.
- Leiman, P. G., Basler, M., Ramagopal, U. A., Bonanno, J. B., Sauder, J. M., Pukatzki, S., Burley, S. K., Almo, S. C. & Mekalanos, J. J. (2009). *Proc. Natl Acad. Sci. USA*, **106**, 4154–4159.
- Lennox, E. S. (1955). *Virology*, **1**, 190–206.
- Matthews, B. W. (1968). *J. Mol. Biol.* **33**, 491–497.
- Planamente, S., Salih, O., Manoli, E., Albesa-Jové, D., Freemont, P. S. & Filloux, A. (2016). *EMBO J.* **35**, 1613–1627.
- Pukatzki, S., Ma, A. T., Revel, A. T., Sturtevant, D. & Mekalanos, J. J. (2007). *Proc. Natl Acad. Sci. USA*, **104**, 15508–15513.
- Pukatzki, S., Ma, A. T., Sturtevant, D., Krastins, B., Sarracino, D., Nelson, W. C., Heidelberg, J. F. & Mekalanos, J. J. (2006). *Proc. Natl Acad. Sci. USA*, **103**, 1528–1533.
- Römling, U., Fiedler, B., Bosshammer, J., Grothues, D., Greipel, J., von der Hardt, H. & Tümmler, B. (1994). *J. Infect. Dis.* **170**, 1616–1621.
- Sauter, N. K., Grosse-Kunstleve, R. W. & Adams, P. D. (2004). *J. Appl. Cryst.* **37**, 399–409.
- Shalom, G., Shaw, J. G. & Thomas, M. S. (2007). *Microbiology*, **153**, 2689–2699.
- Sheldrick, G. M. (2008). *Acta Cryst. A* **64**, 112–122.
- Shneider, M. M., Buth, S. A., Ho, B. T., Basler, M., Mekalanos, J. J. & Leiman, P. G. (2013). *Nature (London)*, **500**, 350–353.
- Silverman, J. M., Agnello, D. M., Zheng, H., Andrews, B. T., Li, M., Catalano, C. E., Gonen, T. & Mougous, J. D. (2013). *Mol. Cell*, **51**, 584–593.
- Studier, F. W. & Moffatt, B. A. (1986). *J. Mol. Biol.* **189**, 113–130.

- Winn, M. D. *et al.* (2011). *Acta Cryst.* **D67**, 235–242.
- Winter, G. (2010). *J. Appl. Cryst.* **43**, 186–190.
- Winter, G. & McAuley, K. E. (2011). *Methods*, **55**, 81–93.
- Yanisch-Perron, C., Vieira, J. & Messing, J. (1985). *Gene*, **33**, 103–119.
- Zhang, Z., Sauter, N. K., van den Bedem, H., Snell, G. & Deacon, A. M. (2006). *J. Appl. Cryst.* **39**, 112–119.
- Zheng, J. & Leung, K. Y. (2007). *Mol. Microbiol.* **66**, 1192–1206.
- Zoued, A., Durand, E., Bebeacua, C., Brunet, Y. R., Douzi, B., Cambillau, C., Cascales, E. & Journet, L. (2013). *J. Biol. Chem.* **288**, 27031–27041.
- Zoued, A., Durand, E., Brunet, Y. R., Spinelli, S., Douzi, B., Guzzo, M., Flaugnatti, N., Legrand, P., Journet, L., Fronzes, R., Mignot, T., Cambillau, C. & Cascales, E. (2016). *Nature (London)*, **531**, 59–63.
- Zoued, A., Durand, E., Santin, Y. G., Journet, L., Roussel, A., Cambillau, C. & Cascales, E. (2017). *Bioessays*, **39**, 1600262.